JOURNAL OF CATALYSIS 121, 441–455 (1990)

Chemisorption and FTIR Study of Bimetallic Pt–Au/SiO_2 Catalysts

K. BALAKRISHNAN, A. SACHDEV, AND J. SCHWANK

Department of Chemical Engineering, The University of Michigan, Ann Arbor, Michigan 48109-2136

Received August 1, 1989; revised September 18, 1989

Pt/SiO_2, Au/SiO_2, and bimetallic $Pt–Au/SiO_2$ catalysts were prepared by incipient wetness impregnation of nonporous SiO_2. The catalysts were characterized after reduction in H_2 by static volumetric chemisorption and infrared spectroscopy. For the monometallic and the bimetallic catalysts, H_2, O_2, and CO were used as adsorbates at room temperature. Additionally, for the monometallic Au/SiO_2 catalyst, O_2 adsorption at 473 K was also used. Infrared spectra of adsorbed CO were obtained on all catalysts. Addition of gold decreased the uptake of all three adsorbates at room temperature, without significantly influencing the relative amounts of weakly held adsorbed species which could be removed upon pumping for 30 min. Agreeing with CO chemisorption data, the total integrated intensity of the linear CO band decreased with increasing Au content. The IR results indicated a predominantly geometric effect of Au causing a shift of the linear CO band to lower wavenumbers. The shift could be rationalized in terms of decreased dipole–dipole coupling of adsorbed CO species. The results are discussed within the context of a previous investigation using electron microscopy, TPR, and reactivity data. Portions of the bimetallic catalysts were subjected to three high-temperature oxidation/reduction cycles and characterized by static chemisorption of H_2 to investigate the effect of this thermal treatment on Pt dispersion.

INTRODUCTION

$Pt–Au/SiO_2$ is a particularly interesting bimetallic catalytic system to study. Au is a poor catalyst compared to Pt, thereby allowing one to assess more clearly the effect of the second metal component. The Pt–Au phase diagram shows a miscibility gap between 18 and 98% Pt (*1*). In this range of composition, one would not expect bulk three-dimensional alloys on supported bimetallic catalyst samples to form (*2*), although the formation of small bimetallic aggregates or "clusters" is conceivable. A detailed study of the microstructure and reactivity of the catalysts used in this work has been presented elsewhere (*3*).

This paper follows up on the microstructural characterization and deals with the adsorption behavior of $Pt–Au/SiO_2$ catalysts. The techniques that we used in this study were chemisorption of H_2, CO, and O_2 at room temperature, and infrared spectroscopy of adsorbed CO. The goal was to learn more about the adsorption behavior of these catalysts with special emphasis on the effect of the addition of the second metal. There have been several previous studies on the Pt–Au system. A general tendency has been found for the segregation of Au to the surface of Pt–Au alloys. This phenomenon has been attributed to the lower heat of sublimation of gold compared to that of platinum. Bouwman and Sachtler (*4*) in their work on vapor-deposited and sintered Au–Pt films found that the gold-rich alloy phase had a lower work function than gold or platinum alone and that the gold-rich phase covered the platinum-rich phase in compositions that fell within the miscibility gap. Sachtler *et al.* (*4, 5*) discovered that for equilibrated Au–Pt films with compositions in the miscibility gap the surface composition would not change and their work functions would be the same. This study also showed that exposure to CO for extended periods of time led to an increase in the amount of platinum on the surface of the film (*4*). The surface enrichment of Pt occurred because Pt chemisorbs CO to a

0021-9517/90 $3.00

much larger extent than Au does, and hence, this configuration would lead to a decrease in surface free energy due to the increased bond formation with CO (*6*). Auger electron spectroscopy on polycrystalline Pt–Au samples containing 2, 5, and 90% Au showed surface segregation of gold in the alloys resulting from the significantly lower surface free energy of Au, even though in the alloy containing 90% Au the heat of solution and elastic strain mismatch data would have predicted otherwise (*7*).

Selective chemisorption of gases on a supported bimetallic catalyst system where one metallic component strongly adsorbs the gas while the other adsorbs either weakly or not at all is a good way to either obtain individual metal dispersions or assess the effect of one metal on the strength of adsorption of a gas on the other metal. The Pt–Au/SiO_2 system is interesting because at room temperature gold alone does not show any significant uptake of H_2 or O_2 while it reversibly adsorbs some small amounts of CO. Platinum, on the other hand, adsorbs significant amounts of H_2, CO and O_2 at room temperature with well-known chemisorption stoichiometries. Supported gold has been found to adsorb O_2 at 473 K with the stoichiometry Au/O = 2 (*8*). In this work we have reported the results of room temperature adsorption of H_2, CO, and O_2 on Pt–Au/SiO_2 catalysts. The use of three different adsorbates provides a larger data base for metallic dispersion. O_2 chemisorption at 473 K has been carried out to determine the average particle size in the case of the monometallic Au/SiO_2 catalyst.

Infrared spectroscopy using CO as adsorbate was used to provide finer details about the influence of gold on the adsorption behavior of CO on Pt sites. IR work has been done on several bimetallic systems containing either Pt or Pd as the primary metal and a host of second metals like Ag, Au, Cu, Pb, Sn, and Re. One objective of these studies was to determine whether there are ensemble effects, ligand effects, or both present as a result of addition of the second metal. Kugler and Boudart (*9*) found indications of both ligand and ensemble effects in their work on small palladium–gold alloy particles. The high-frequency CO adsorption bands on Pd (above 2000 cm^{-1}) shifted to lower wavenumbers with increasing Au content. This was attributed to a ligand effect as surface coverage did not affect the position of these bands. On the other hand, the band intensity of the irreversibly adsorbed CO increased with increasing Pd content and this was attributed to an ensemble effect. Somo-Noto and Sachtler (*10*) in their study on Pd–Ag alloys found that the intensity of the linearly adsorbed CO increased relative to the bridge-bonded species on alloying Pd with Ag, giving evidence for a geometric effect. Hendrickx and Ponec (*11*) used isotopic dilution and found that the Pd–Cu alloy system did not show any measurable ligand effect while the Pd–Ag system showed some effect, although it was not very large. Ponec and coworkers (*12, 13*) have studied supported catalyst systems containing Pt alloyed with other metals. Their results showed a decrease in the adsorption band frequency for CO linearly adsorbed on Pt by alloying with Pb, Sn, Re, or Cu, but only for Pb was there any evidence of an electronic effect over and above the geometric effect. Palazov *et al.* (*14*) also suggested that in the supported Pt–Pb system there are both geometric and electronic effects which can modify the reactivity of the system. A detailed adsorption study of the Pt–Ag/SiO_2 alloy system was performed by De Jong *et al.* (*15*). They found that CO was adsorbed in linear fashion on Pt sites and that dilution of the Pt sites with Ag led to a shift of the IR band to lower wavenumbers.

These and other results encouraged us to take a closer look at the Pt–Au/SiO_2 system. The catalysts studied were monometallic Pt/SiO_2, monometallic Au/SiO_2, and two bimetallic catalysts having 17 and 30 at.% Au, so that their bulk compositions lay in the region of the miscibility gap in the Pt–Au phase diagram. A blank silica sam-

ple was examined under similar experimental conditions to assess any effects of the support alone. The catalysts were prepared and pretreated using techniques generally used for dispersed metal catalysts and no attempt was made to deliberately create alloys or solid solutions. The reactivity and microstructure data of these catalysts as detailed in Ref. (*3*) showed that the catalyst with 17 at.% Au had a lower selectivity to isomerization products in *n*-hexane conversion reactions compared to that of the monometallic Pt/SiO_2 catalyst, while the catalyst containing 30 at.% Au behaved in the opposite way. This difference in the reactivity was also highlighted in the TPR and the microscopy results which indicated closer interaction between Pt and Au in the case of the catalyst having 30 at.% Au. In light of these results we felt it was necessary to attempt to understand better the role of Au in modifying the catalytic surface. Hence, chemical probes such as gas chemisorption and infrared spectroscopy of adsorbed CO were chosen as additional characterization tools.

EXPERIMENTAL

I. Catalyst Preparation

The nominal catalyst loadings are shown in Table 1 including the actual metal compositions as determined by neutron activation analysis. The silica support used was nonporous Degussa aerosil 200 (BET surface area = 200 m^2/g). The composition in wt% as specified by the manufacturer was $SiO_2 > 99.8$, $Al_2O_3 < 0.05$, $Fe_2O_3 < 0.003$, $TiO_2 < 0.03$, $HCl < 0.025$, and sieve residue <0.05. The platinum precursor was hydrogen hexachloroplatinate (IV) hydrate containing 39.7% Pt and the gold precursor was hydrogen tetrachloroaurate trihydrate with a gold composition of 50% (Aldrich Chemicals). The monometallic samples were prepared by impregnation of the support with aqueous solutions of the metal precursors using the method of incipient wetness. The bimetallics were coimpregnated using the same technique. The impregnation was followed by a drying step at 393 K in flowing high-purity air. All samples were prereduced in flowing hydrogen (ultrahigh purity) for 14 h at 673 K.

II. Chemisorption

The chemisorption experiments were performed in an all-glass static volumetric high-vacuum system with two liquid nitrogen-cooled traps preventing backstreaming of pump fluids. The system had two pressure gauges: an MKS Baratron Type 122A pressure gauge with two capacitance manometers (0–10 Torr, 10–1000 Torr range) and a calibrated Veeco ionization gauge to measure pressure in the 10^{-3} to 10^{-6} Torr

TABLE 1

Catalyst Composition and Chemisorption Results

Catalyst nominal wt%	Metal wt%	Au atom%	Gas uptake (cc STP/g catalyst)				
			Hydrogen		Oxygen (total)	CO	
			Total	% Weak		Total	% Weak
1.0 Pt	1.00	0	0.383	35	0.261	0.574	9
1.0 Pt–0.3 Au	1.39	17	0.182	40	0.133	0.273	11
1.0 Pt–0.7 Au	1.58	30	0.087	38	0.067	0.134	10
2.0 Au	1.25	100			0.040[a]		

[a] Irreversible uptake at 473 K corrected for adsorption on support.

range (1 Torr = 133.3 Pa). Research-grade gases stored in Pyrex glass bulbs were used for the experiments. The temperature of the adsorption zone was controlled to about 1 K accuracy.

The pretreatment protocol consisted of room temperature evacuation for 20 min, heating to 673 K in about 40 min, and evacuation at 673 K for 4 h to remove water and other adsorbed impurities. Then, the reduction was started in 250 Torr of static hydrogen. After 12 h, the sample loop was evacuated at 673 K for 30 min. A second dose of 250 Torr hydrogen was admitted to the sample and kept there for 2 h, followed by a high-temperature evacuation at 678 K for 9 h at pressures close to 1×10^{-5} Torr. Then the sample was cooled to room temperature under dynamic vacuum to collect adsorption isotherm data.

Each set of isotherms consisted of a total uptake isotherm and an isotherm to determine weakly adsorbed gas. After the first isotherm the sample was evacuated at the same temperature for 30 min and a second isotherm was obtained. The difference between these two isotherms gave us the strongly held gas at a given temperature after 30 min evacuation. This definition of irreversible adsorption on Pt–Au/aerosil has been used before by Anderson *et al.* (*16*). The equilibrium pressures in our experiments were typically in the 0–12 Torr range. For the room temperature isotherms sufficient time was allowed for equilibration before collecting data points. Each isotherm consisted of six or more points. The method of extrapolation of the linear region of the isotherm to zero pressure was used to get the uptake of gas on the sample. In the case of the bimetallics this same procedure has been adopted and the same stoichiometry of adsorption has been used as would be used for monometallic Pt/SiO_2. The validity of this method has been verified for hydrogen adsorption by Anderson *et al.* (*16*).

After collecting hydrogen chemisorption data at room temperature, the sample was heated to 678 K, evacuated for 9 h, and then cooled to room temperature for CO chemisorption. Subsequently, to remove the adsorbed CO, the sample was heated to 673 K under dynamic vacuum and evacuated for 4 h. It was then reduced for 4 h and again subjected to high-temperature evacuation. After cooling to room temperature under dynamic vacuum, O_2 chemisorption was carried out. After the chemisorption experiments, the dead volume of the reactor loop was determined by expanding helium.

Besides room temperature isotherms, O_2 adsorption experiments were also carried out at 473 K on the monometallic 2.0 Au/SiO_2 catalyst. For this purpose, the sample was again reduced and evacuated at the same temperatures as before and then cooled to 473 K under dynamic vacuum. The uptake of O_2 was measured in single-point experiments. The rationale for this was that slow uptake of O_2 at 473 K has been reported for Au-containing catalysts earlier (*8*). This slow uptake was attributed to diffusion of oxygen species onto the support. Hence, it was decided to use a single-point isotherm where data points were collected at various times after introducing around 8.5 Torr of O_2 into the reactor loop. The drop in pressure was monitored until there was no significant change in pressure as a function of time. A second single-point isotherm was collected after 30 min evacuation at 473 K. The difference between the values obtained by extrapolating the linear region of the isotherms to zero time was used to calculate the amount of irreversibly adsorbed O_2. After the experiments, helium was expanded at 473 K to determine the correction factor for the dependency of pressure on temperature.

After completion of all the chemisorption experiments as outlined above, the two bimetallic samples were "alloy equilibrated" adapting a method proposed by Anderson *et al.* (*16*). This consisted of three alternating cycles of oxidation (O_2, 573 K, 5 h) and reduction (H_2, 620 K, 16 h). Between expo-

sure to gas, the samples were evacuated for 30 min at the pretreatment temperature. After the oxidation/reduction cycles, the sample was evacuated for 9 h at 678 K and then was allowed to cool to room temperature before hydrogen chemisorption isotherms were performed to determine if there was any difference in the uptake and the shape of the isotherm compared to those of the bimetallic samples which had been subjected to prereduction only.

III. Infrared Spectroscopy

Two kinds of IR cells were used in this work. One cell was a stainless-steel cell similar in design to that used by Robbins (*17*). The central cell body consisted of a $2\frac{3}{4}$-in. Conflat flange with two holes with $\frac{1}{4}$-in. stainless-steel tubes welded onto the metal on the inside. A third hole was drilled to pass a thermocouple inside. Sapphire viewports (MDC) with Kovar sleeves attached to stainless-steel flanges were used as IR windows. This cell could be heated to 673 K and a vacuum of 1×10^{-5} Torr could be easily achieved.

To avoid any possible metal contamination or metal carbonyl formation, a special IR cell was designed in our lab which had the capacity to operate at high temperatures of about 873 K under a vacuum of 10^{-5} Torr or below. The cell body was made of quartz. Sodium chloride windows (Wilmad, 38 × 6 mm) were sealed to the cell body with Viton O-rings, secured with heat-shrinkable tubing and custom-machined metal flanges pressing against the windows. Holes were drilled in the flanges and a copper water-cooling jacket was inserted. An additional cooling jacket was mounted on the cylinder near the windows to ensure that the heat-shrink tubing and the windows never got very hot. The IR pellet was mounted on a quartz sample holder and placed in the heated zone in the center of the cell. This zone was heated by using a well-insulated beaded heating wire wrapped around the outside of the cell. A thermocouple was inserted into a thermowell on top of the pellet. The temperature was controlled using an Omega temperature controller. A thermocouple gauge was connected to the IR cell to monitor pressures in the range 1–1000 mTorr. An ionization gauge was used to measure pressures lower than 10^{-3} Torr. The IR cell could be isolated from the vacuum and gas lines with vacuum stopcocks. The gases used for the infrared experiments were all research grade. The vacuum in the IR cell was provided by an air-cooled oil diffusion pump and a mechanical pump. Backstreaming of pump oil was prevented by a liquid nitrogen baffle on top of the diffusion pump and a liquid nitrogen trap between the foreline and the mechanical pump.

The infrared spectrometer was a Digilab FTS 20/C FTIR interfaced to a Nova-4 X computer and all spectra were collected at a resolution of 2 cm^{-1}. At this resolution, signal averaging of 256 scans gave an acceptable signal-to-noise ratio. The pretreatment procedure of catalyst powders for IR experiments consisted of the following steps: 80 mg of prereduced sample was pressed into a thin wafer between 1-in. stainless-steel dies at 4000 psi for 1 min. After mounting the pellet in the cell, the cell was evacuated and the temperature was raised to 673 K and kept under dynamic vacuum for 4 h. The catalyst pellet was reduced for 8 h under H_2. Then, the cell was evacuated at 678 K until a dynamic vacuum of at least 1×10^{-5} Torr was reached, and the temperature was lowered to 298 K.

After collecting a reference spectrum at 298 K, the pellet was heated to 493 K, and a second reference spectrum was collected. The main reason for choosing this temperature was that the bridge-bonded species of adsorbed CO on a 1% Pt/Al_2O_3 sample has been found to appear more clearly at higher temperatures (*18*) and the relative intensity of IR bands due to linear vs bridge-bonded CO species is a good indicator for the effect of diluting Pt ensembles with a second metal. Once the reference spectrum at 493 K had been recorded, the pellet was ex-

posed to 1 atm of CO for 20 min (1 atm = 101.3 kPa). The rationale for using 1 atm of CO at high temperatures has been explained by Haaland (*18*). He found that at 460 K there was a significant increase in adsorption of CO on 1% Pt/Al_2O_3 when the partial pressure of CO was increased from 76 Torr to 1 atm.

After 20 min of exposure to 1 atm of CO, the CO gas pressure was lowered to 5 Torr and a spectrum was collected at 493 K. The reason for decreasing the gas-phase pressure to 5 Torr before collecting the spectra was to better observe the adsorption bands, if any, on Au sites, known to weakly adsorb CO (*19*). The cell was allowed to cool to room temperature with CO gas inside, and a spectrum was collected. Then, the pellet was again exposed to a dose of 1 atm of CO, this time at room temperature. In the case of the Au/SiO_2 sample, spectra were collected after reducing the CO pressure to 5 Torr and further to 1 Torr. For all samples, additional spectra were collected immediately after removal of the gas phase and after evacuation with the diffusion pump at room temperature.

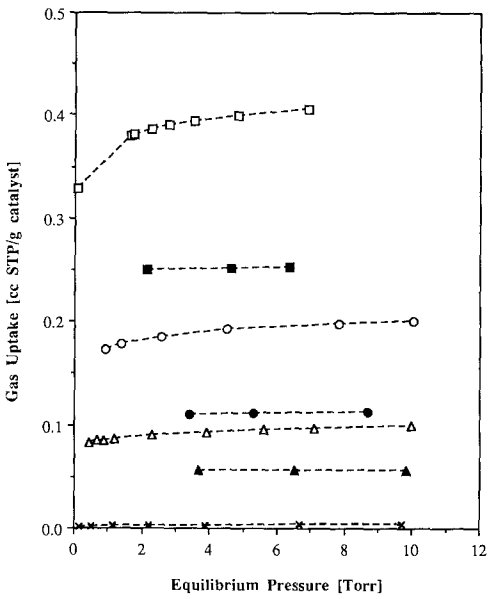

FIG. 1. Room temperature hydrogen chemisorption isotherms for catalysts of the $Pt–Au/SiO_2$ series. (□) 1.0 Pt/SiO_2 (total); (○) 1.0 Pt–0.3 Au/SiO_2 (total); (△) 1.0 Pt–0.7 Au/SiO_2 (total); (x) 2.0 Au/SiO_2 (total); (■) 1.0 Pt/SiO_2 (strong); (●) 1.0 Pt–0.3 Au/SiO_2 (strong); and (▲) 1.0 Pt–0.7 Au/SiO_2 (strong). Strongly adsorbed gas is defined as the amount of gas remaining on the catalyst surface after 30 min evacuation at room temperature.

RESULTS AND DISCUSSION

I. Chemisorption at Room Temperature

(*1*) *Hydrogen.* Hydrogen chemisorption is a good probe for exposed platinum atoms in the catalysts as gold atoms have not displayed the capacity to dissociate molecular hydrogen at room temperature (*20–23*). The hydrogen chemisorption isotherms obtained on our catalyst series are displayed in Fig. 1. The total uptakes including weakly adsorbed hydrogen (as defined under Experimental) are summarized in Table 1.

The blank silica showed a hydrogen uptake which was negligibly small compared to that of the Pt-containing catalysts. Since the isotherm passed through the origin on back-extrapolation to zero pressure, the gas was probably physically adsorbed. Evacuation led to the desorption of most of this adsorbed gas. The monometallic Au/SiO_2 catalyst showed an uptake of hydrogen that was about double that of the blank silica. There was some indication of chemisorption although it was less than 1% of the amount chemisorbed on the monometallic Pt/SiO_2 catalyst.

The monometallic 1.0 Pt/SiO_2 catalyst showed a total uptake of 0.383 cc STP/g of catalyst corresponding to a Pt dispersion (H/Pt_{total}) of 0.67 assuming an adsorption stoichiometry of $H/Pt_{surface} = 1$. Total hydrogen uptake at room temperature has been used to determine the Pt surface atoms for the $Pt–Au/SiO_2$ catalysts as suggested by Anderson *et al.* (*16*). In the bimetallic catalyst 1.0 Pt–0.3 Au/SiO_2, the addition of 17 at.% Au caused a decrease in the H/Pt_{total} ratio to 0.28. On further increasing the amount of Au to 30 at.% (cata-

lyst 1.0 Pt–0.7 Au/SiO_2), there was a decrease in the H/Pt_{total} ratio to 14%. These ratios were derived by assuming that at room temperature all the H_2 was adsorbed on the Pt surface sites of Pt–Au/SiO_2 catalysts. The decrease in Pt dispersion with addition of Au has been observed before (*2*). This is unlike the result obtained in the Ru–Au/SiO_2 system, having metallic components that are completely immiscible in the bulk state, where addition of gold did not change the amount of exposed Ru (*24*).

In the Pt system, it was observed that the trends in the strongly adsorbed hydrogen, as defined under Experimental, were similar to the total H_2 adsorption. There was no significant difference in the percentage of weakly adsorbed H_2 with increasing amounts of gold in the three catalysts. Typically, 35–40% of the H_2 adsorbed could be desorbed by pumping at room temperature for 30 min. Other researchers have seen in chemisorption experiments at room temperature on supported Pt the presence of weakly held hydrogen (*16, 25*). Temperature-programmed desorption (*26, 27*) and infrared spectroscopy (*28, 29*) have detected on Pt surfaces the presence of several forms of adsorbed H_2, some of it weakly held.

Another interesting point was the shape of the hydrogen chemisorption isotherms at room temperature on our bimetallic Pt–Au/SiO_2 catalysts. Anderson *et al.* (*16*) had noted that bimetallic Pt–Au/SiO_2 catalysts having gold contents of 33 and 85 at.%, respectively, showed H_2 uptakes that did not saturate. The reason given for this was the possibility of a spillover effect of hydrogen from the Pt onto the Au sites. In our case we found nearly linear isotherms in all the Pt-containing samples including the sample containing 30 at.% Au. Saturation was reached at around 6–8 Torr (1 Torr = 133.3 Pa) equilibrium pressure.

It was then decided to put our bimetallic samples through three oxidation–reduction cycles. The details are given under Experimental. This oxidation–reduction cycling process had been used before as a means of equilibrating the alloy surface in the supported Pt–Au system (*16, 30*). After these cycles, H_2 chemisorption at room temperature showed that although there was no notable change in the shape of the isotherms, there was an increase in total hydrogen uptake by about 14% in the case of the catalysts having 17 at.% Au while there was no significant change in the uptake on the 30 at.% Au catalyst. This suggests that in the latter sample the oxidation–reduction cycling did not significantly change the catalytic surface. The slight increase in H_2 uptake seen for the 17-at.% Au catalyst could be due to a certain degree of redistribution of Pt in this catalyst. Compared to Pt–Au/Al_2O_3, Pt–Au/SiO_2 catalysts tend to be less susceptible to redispersion as long as there is a close proximity of Pt and Au, as evident from the work of De Jongste and Ponec (*31*). For redispersion to occur on a silica-supported sample, the presence of segregated Pt particles seems to be a prerequisite. The results of a previous EDX analysis (*3*) confirmed that in the catalyst having 17 at.% Au the Pt and Au particles were segregated, justifying the observed change in Pt dispersion upon oxidation–reduction cycling. In the 30-at.% Au catalyst the two metals appeared to be in close proximity forming bimetallic aggregates, and this catalyst did not show any detectable change in dispersion when subjected to the cycling routine.

The chemisorption average particle size obtained for the 1.0 Pt/SiO_2 catalyst was 1.52 nm, assuming a spherical particle shape. The average area occupied by one Pt surface atom was assumed to be 0.089 nm^2 (*32*). On the basis of electron microscopy (*3*) a number average particle diameter value, d_n = 3.72 nm, and a surface average diameter, d_s = 6.75 nm, were obtained. Generally, one would expect the surface average diameter, d_s, to match the average particle size determined from chemisorption. The reason for the discrepancy is twofold. First, the particle sizes for this cata-

lyst were not normally distributed and the electron micrographs showed some as large as 16 nm. A few particles on the larger side of the distribution can substantially increase the surface average diameter obtained from microscopy. Secondly, the micrographs showed the presence of nonspherical, elongated particles. The formation of such nonequilibrium shapes could result from the combination of smaller particles during reduction or from the nonporous nature of the support. The bimetallic catalysts had a larger particle size range than the monometallic Pt/SiO_2 catalyst, varying from 0.5 to 40 nm with d_n = 4.95 nm for the 17-at.% Au catalysts and 4.44 nm for the 30-at.% Au sample. EDX analysis showed that in the 17-at.% Au sample the metal particles smaller than 20 nm were mainly Pt while the larger particles (>20 nm) were composed mostly of monometallic Au. But, for the 30-at.% Au catalyst EDX indicated that Pt and Au coexisted within individual metal particles almost in the entire particle size range. Most of the metal particles in the size range up to 10 nm had the Au_3Pt composition (*3*).

The chemisorption results do not tell anything about the particle size distribution and cannot be used to obtain the average particle size for the bimetallic catalysts. However, chemisorption clearly showed a steady decline in the amount of Pt exposed with increasing gold content. One possible explanation for this could be that in the 17-at.% Au sample small amounts of Au could be sitting on top of the Pt particles thereby blocking the sites for chemisorption. Submonolayers of Au decorating the surface of a Pt particle could be below the detectable limit of EDX. Another explanation for the decreased Pt dispersion could be that during catalyst preparation some Pt nucleation sites on the support are blocked by Au, forcing Pt to form larger particles. In the 30-at.% Au sample, EDX confirmed that Au and Pt coexist within individual particles. The decrease in Pt dispersion could be due to the surface segregation of Au. In this context, it is interesting to compare the Pt–Au/SiO_2 system with Pt–Ag/SiO_2 where no significant surface enrichment in Ag was found after reduction and evacuation (*15*).

(2) *Carbon monoxide.* The plain silica showed some CO uptake which was completely reversible and extremely small compared to that of the Pt-containing catalyst. There was no indication of any chemisorption from back extrapolation of the isotherm to zero pressure. In the monometallic 2.0 Au/SiO_2 catalyst there was some evidence of chemisorption corresponding to less than 1% of the CO uptake on 1.0 Pt/SiO_2. The CO uptake on 2.0 Au/SiO_2 was fully reversible in the equilibrium pressure range of 0–4 Torr, but there seemed to be a slight irreversibility starting at higher pressures. The monometallic 1.0 Pt/SiO_2 catalyst showed a total uptake of 0.574 cc STP/g of catalyst. It is relevant to mention here that in our study the infrared spectroscopy results showed that most of the CO was adsorbed in the linear mode at room temperature on the platinum-containing catalysts. There was no evidence of the presence of any significant amounts of bridge-bonded CO species. This is consistent with the observation that on silica-supported Pt there is less likelihood for the formation of bridge-bonded CO species compared to alumina-supported Pt (*33*).

For the bimetallic Pt–Au/SiO_2 catalysts the trends of CO total uptake were similar to the total hydrogen uptake, i.e., there was a decrease in CO uptake with increasing Au at.% (Table 1). The decrease in CO adsorption with increasing gold can be simply attributed, analogous to hydrogen adsorption, to a decreased number of Pt sites exposed resulting from gold segregation to the surface. It was found that the percentage of weakly adsorbed CO was around 10% in the Pt-containing catalysts. The method of subtracting two isotherms to get strongly adsorbed CO has been used before (*34*). Another observation in the platinum catalysts was that the total CO uptake was lower than the total hydrogen atom uptake.

For the 1.0 Pt/SiO_2 sample, the CO/Pt_{total} ratio was only 0.5 compared to the H/Pt_{total} ratio of 0.67 and the O/Pt_{total} ratio of 0.46. This would lead to discrepancies in calculation of Pt dispersion, depending on the adsorbate chosen. If, on the other hand, only the strongly adsorbed CO or H_2 were used, then the calculated CO/Pt_{total} ratio becomes 0.46, and the H/Pt_{total} ratio is 0.43, in good agreement with the O/Pt_{total} ratio.

(*3*) *Oxygen.* The blank silica showed some minute oxygen chemisorption, most of it weakly held. The monometallic 2.0 Au/SiO_2 catalyst showed about three times the total uptake of the blank silica with some irreversible adsorption. This could have been due to adsorption on the Au sites, though it cannot be ruled out that trace amounts of impurities in the catalyst contributed to this uptake.

In contrast to H_2 and CO adsorption, there were no significant amounts of weakly chemisorbed oxygen species observed. Total O_2 uptake was used to calculate the number of exposed Pt sites assuming a stoichiometry of $O/Pt_{surface} = 1$. The O_2 uptake for the 1.0 Pt/SiO_2 catalyst was 0.261 cc STP/g catalyst which corresponds to an O/Pt_{total} value of 0.46. This uptake value decreased with increasing Au at.% (Table 1). Hence, oxygen chemisorption is a good indicator of exposed Pt sites, but it tends to give a lower value for monolayer coverage compared to hydrogen chemisorption. Wilson and Hall (*35*), on the basis of electron microscopy results and a detailed study of H_2 and O_2 chemisorption on Pt/Al_2O_3, concluded that H_2 chemisorption was more indicative of the Pt surface area. When the dispersion was low, they found O_2 uptake values close to the H_2 uptake. But when the dispersion was high O_2 uptake tended to be lower than the H_2 uptake. Palmer and Vannice (*25*) in chemisorption studies on Pt/SiO_2 samples found that in most cases the H_2 uptake was higher than the O_2 uptake, but they did not find any definite relationship between adsorption stoichiometry and particle size. They used X-ray diffraction data on Pt/C catalysts to show that hydrogen chemisorption was a more sensitive judge of particle size than oxygen chemisorption. In our case we noted that the O_2 uptake was lower than the H_2 uptake. For the reasons mentioned earlier, we believe that H_2 chemisorption at room temperature is a good indicator of Pt dispersion, but the presence of weakly adsorbed H_2 species complicates the analysis.

Oxygen chemisorption at elevated temperatures has been used before to determine the dispersion of Au. There has been controversy in the literature concerning the phenomenon of O_2 adsorption on bulk and supported Au surfaces. A chemisorption stoichiometry of Au/O = 2 for O_2 adsorption on Au/SiO_2 at 473 K has been confirmed by Fukushima *et al.* (*8*) who used XRD and TEM results in conjunction with chemisorption data. This stoichiometry changed to Au/O = 1 on raising the temperature to 573 K. They also found that in a 2.0 Au/MgO catalyst there was insignificant reversible O_2 adsorption at 473 K, but on raising the temperature to 673 K almost all the O_2 adsorption was reversible.

The details of the experiments and the reason for using single-point chemisorption have been detailed under Experimental. Two successive isotherms were run separated by a 30-min evacuation to determine the irreversible uptake. The blank silica showed some small uptake but it leveled off after less than an hour. The monometallic 2.0 Au/SiO_2 catalyst showed an initial rapid uptake followed by some slow uptake persisting to even 3 h after the start of the isotherm. This effect had been observed by Fukushima *et al.* (*8*) and had been attributed to a diffusion onto the silica support. A second isotherm was collected after 30 min evacuation at 473 K. Some reversible uptake of O_2 was found corresponding to about 16% of the total uptake. The difference between the two uptake values was calculated and then corrected for the irreversible adsorption on the blank silica to get values for O_2 irreversibly adsorbed on gold.

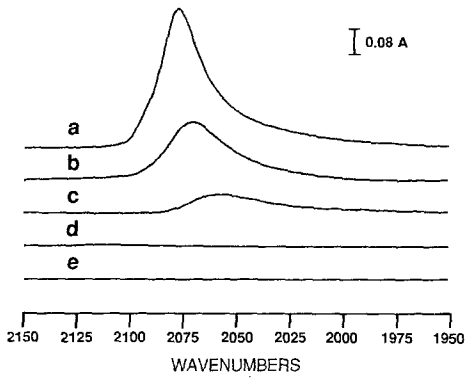

FIG. 2. IR spectra of linearly adsorbed CO at 298 K. (a) 1.0 Pt/SiO_2, (b) 1.0 Pt–0.3 Au/SiO_2, (c) 1.0 Pt–0.7 Au/SiO_2, (d) 2.0 Au/SiO_2, and (e) blank SiO_2. These spectra were obtained after removal of gas-phase CO.

The corrected adsorption value of 0.040 cc STP/g catalyst for the 2.0 Au/SiO_2 catalyst was used to calculate the average particle size of gold assuming a spherical particle shape. A cross-sectional area of 0.0913 nm^2 per surface Au atom (*36*) was assumed. The average particle size was 10.1 nm while microscopy results (*3*) had given values of the number average particle size, d_n = 12.6 nm, and surface average particle size, d_s = 15.9 nm.

II. Infrared Spectroscopy

An overview of the IR spectra obtained on the various catalysts of the Pt–Au series after exposure to CO at room temperature is given in Fig. 2. The blank silica pellet showed no significant peak due to adsorbed species in the region of interest (2200–1700 cm^{-1}), both at 493 K, which was the temperature at which the sample was initially exposed to CO, and at 298 K.

Figure 3 illustrates the behavior of the IR peaks on 1.0 Pt/SiO_2 as a function of the history of exposure to CO as detailed under Experimental. The monometallic 1.0 Pt/SiO_2 catalyst showed a strong peak at 2070 cm^{-1} after exposing the catalyst pellet to CO at 493 K and decreasing the gas-phase pressure to 5 Torr. On cooling to 298 K, the peak shifted to 2077 cm^{-1} and the peak height increased by 18%. This peak shift can be attributed to a higher surface coverage of CO at 298 K than at 493 K. Haaland (*18*) had earlier observed that CO adsorption bands on 1.0 Pt/Al_2O_3 shifted to higher frequencies when the adsorption temperature was lowered. On adding a second dose of CO to our sample at 298 K and evacuating the gas phase, the peak position did not change. The band at 2077 cm^{-1} can be assigned to CO linearly adsorbed on fully reduced Pt sites, in agreement with the literature. On evacuating at 298 K for 30 min, we found that the peak position of linear CO on Pt shifted to a lower frequency of 2073 cm^{-1} and the total integrated band intensity decreased by around 9%. This result matches up well with our room temperature chemisorption data where we noted that about 9% of the total CO adsorbed could be desorbed by a 30-min evacuation. The peak shift to lower frequencies is due to the decreasing coverage of CO on the surface.

Significant amounts of bridge-bonded species were not obtained. The absence of bridge-bonded species at 298 K on a 5% Pt/SiO_2 catalyst has been reported earlier (*37*). In contrast to our IR results on the 1% Pt/

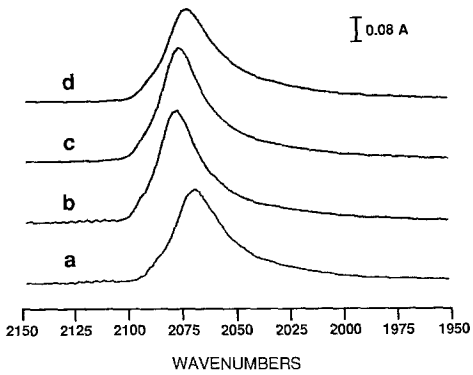

FIG. 3. IR spectra, showing the linearly adsorbed CO peak on 1.0 Pt/SiO_2 catalyst as a function of the CO treatment protocol, collected after the following steps: (a) exposure to CO at 493 K and reduction of gas-phase pressure to 5 Torr; (b) cooling to 298 K under static CO gas; (c) addition of fresh CO at 298 K and evacuation of gas-phase CO; and (d) evacuation at 298 K for 30 min.

SiO_2 catalyst, Barth *et al.* (*38*) found that CO adsorption on a 1% Pt/Al_2O_3 sample resulted in bridge-bonded CO species giving rise to a broad peak at around 1800 cm^{-1}. In the linear region, a peak at 2060 cm^{-1} having a shoulder at 2078 cm^{-1} was obtained. The shoulder can be attributed to CO linearly attached to Pt terraces, while the peak at 2060 cm^{-1} is due to CO linearly adsorbed on steps and corners (*18*). The fact that on our Pt/SiO_2 catalyst only one CO band at 2077 cm^{-1} was observed suggests the predominance of terrace sites. These differences indicate an intriguing possibility that the support and the method of preparation can influence the morphology and surface faceting of platinum particles.

After the room temperature adsorption of CO, the 1.0 Pt/SiO_2 sample was evacuated at 673 K to remove the adsorbed CO. Then, the catalyst pellet was exposed to 760 Torr of static oxygen (research grade) for 90 min at 673 K and cooled to 298 K with the oxygen in the cell. At 298 K, the gas-phase oxygen was removed and a reference spectrum was collected. A dose of CO gas (760 Torr, 20 min exposure time) was introduced into the IR cell and subsequently the gas-phase CO was evacuated before collecting a spectrum. Figure 4 gives a comparison of the IR bands on reduced and oxidized Pt/SiO_2.

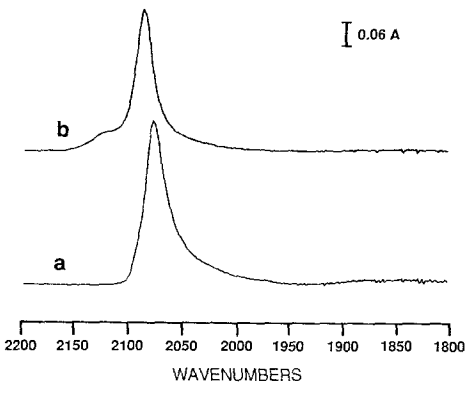

FIG. 4. Comparison of IR spectra of fully reduced and oxidized 1.0 Pt/SiO_2 catalyst obtained at 298 K after removal of gas-phase CO. (a) Fully reduced and (b) oxidized.

The spectrum of the oxidized pellet showed a band at 2087 cm^{-1} with a prominent shoulder at 2120 cm^{-1}. The shoulder at 2120 cm^{-1} can be assigned to coadsorption of a CO and an oxygen atom on the same Pt site (*39*). The peak at 2087 cm^{-1} can be assigned to CO linearly adsorbed on Pt sites that have been modified by nearby oxygen atoms, causing the peak to shift by 10 cm^{-1} to higher frequencies. This shift has been attributed to a compression of the adlayers of CO due to the presence of oxygen. The adlayer compression would increase the dipole–dipole coupling between adsorbed CO atoms resulting in a shift to higher frequencies (*40*). Stoop *et al.* (*41*) used isotopic dilution experiments to show that this increase in frequency of the CO adsorption band because of preadsorbed oxygen was mainly a geometric effect, though a small electronic effect cannot be ruled out. This oxidation experiment convinced us that we do have a fully reduced Pt surface after our reduction and evacuation protocol. It is important to establish a reliable experimental protocol that assures complete reduction of Pt, so that the comparison between monometallic and bimetallic catalyst becomes more meaningful.

The monometallic 2.0 Au/SiO_2 did not show any CO adsorption peak after adding CO at 493 K and lowering the gas-phase pressure to around 5 Torr. On cooling to 298 K in the presence of gas-phase CO there was a slight intensity increase in the low-frequency branch of the gas-phase spectrum of CO, suggesting a superimposed peak of adsorbed CO. Addition of a fresh dose of CO at room temperature and lowering the gas-phase pressure to 5 Torr did not alter the spectrum to any significant degree. On decreasing the gas-phase pressure to 1 Torr, the peak hidden within the low-frequency branch of the gas-phase CO spectrum became more noticeable. After removing the gas-phase with the roughing pump, so that the rotational fine structure of gas-phase CO had totally disappeared, a residual peak was clearly visible at 2112

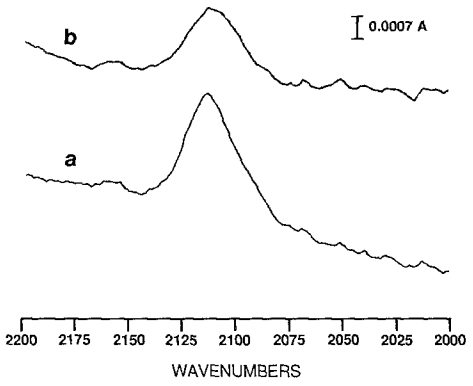

FIG. 5. IR spectra of CO adsorbed on 2.0 Au/SiO_2 catalyst at 298 K. (a) After addition of CO and removal of gas phase and (b) after evacuation at 298 K for 30 min.

cm^{-1} (Fig. 5). The spectra shown in Fig. 5 have been smoothed out as the original spectra were very noisy due to the low absorbance values of the peaks. The total integrated intensity of this peak was less than 1% of the corresponding value obtained for the CO band on the monometallic 1.0 Pt/SiO_2 catalyst (Fig. 2). The peak at 2112 cm^{-1} can be assigned with fair certainty to CO adsorbed on reduced Au sites, in agreement with previous IR studies of CO adsorption on Au. Kottke *et al.* (*42*) in their study of an evaporated gold film at room temperature found a CO adsorption band shifting within the range of 2120–2116 cm^{-1} depending on coverage. Yates (*43*) studied CO adsorption at room temperature on 10 wt% Au supported on Cabosil and found a band at 2116 cm^{-1} when the Au surface was fully reduced. He also found that by evacuating for 1 min at room temperature the CO could be removed from the Au adsorption sites. In our case, even after 30 min of evacuation at 298 K the CO adsorption band did not completely disappear but decreased in intensity by about 40% and shifted from 2112 to 2114 cm^{-1}. Such an increase in the frequency of the CO adsorption band on Au sites as a result of decreasing surface coverage is a characteristic of group IB metals and has been observed before (*19, 42, 43*).

CO adsorption on the bimetallic 1.0 Pt–0.3 Au/SiO_2 catalyst containing 17 at.% Au at 493 K gave an adsorption band at 2060 cm^{-1}. On cooling to 298 K, the peak shifted to 2073 cm^{-1}. After exposure to a fresh dose of CO at 298 K and evacuation of the gas phase, the peak position was 2072 cm^{-1} (Fig. 2). The peak height and total integrated peak area of this band were only 42 and 46%, respectively, of the corresponding band for the monometallic 1.0 Pt/SiO_2.

For the bimetallic 1.0 Pt–0.7 Au/SiO_2 catalyst (30 at.% Au), the CO adsorption peak at 493 K appeared at 2050 cm^{-1} and it shifted to 2060 cm^{-1} on cooling to 298 K. Fresh CO addition and evacuation of the gas phase did not change the position of the band. The peak height of this band was only around 13% of that observed on the monometallic 1.0 Pt/SiO_2 catalyst (Fig. 2). The total integrated peak area also decreased significantly and was about 20% of the peak seen on the 1.0 Pt/SiO_2 sample. No detectable peak resulting from CO adsorption on Au sites was observed on the bimetallic catalysts. The main reason for this might be that the amount of Au in these catalysts was too low to produce any detectable CO adsorption band.

There could be several reasons for the observed shift of the linear CO adsorption peak on reduced Pt sites to lower frequencies with increasing amount of Au. First, the peak shift could be due to a decrease in the average particle size of Pt as a function of increasing Au content. Solomennikov *et al.* (*44*) had observed a shift to higher frequencies of CO adsorption bands on reduced Pt/SiO_2 and Pt/Al_2O_3 catalysts by increasing the temperature of reduction from 673 K to higher values, resulting in a decrease in Pt dispersion. The main reason given for this peak shift was a geometric effect caused by the increased coordination number of the surface Pt atoms with decreasing dispersion. This would lead to a lower degree of π bonding between adsorbed CO molecules and surface metal atoms and consequently, lead to an increase

in the C–O binding energy, according to the concept of backdonation developed by Blyholder (*45*). Toolenaar *et al.* (*46*) studied on Ir/Al_2O_3 the effect of the metal particle size on CO adsorption and found an increase in band frequency with an increase in average particle size. This effect was attributed to a decrease in the strength of exchange of electrons of CO with metal atoms. Earlier microscopy results (*3*) on our samples showed that the number average particle sizes of the bimetallic catalysts were larger than that of the monometallic 1.0 Pt/SiO_2 catalyst. Also, chemisorption results indicated a decrease in Pt dispersion with increasing Au content. Hence, the observed shift to lower wavenumbers with increasing amounts of Au in our catalysts cannot be attributed to a decrease in particle size.

Secondly, the change in frequency could be attributed to a geometric effect because of the presence of Au atoms which would dilute the Pt sites, thereby decreasing the effect of dipole–dipole coupling between adsorbed CO molecules. This dilution would lead to a red shift in the frequency of adsorbed CO as was observed in our study. A similar result was reported by Toolenaar *et al.* for the alumina supported Pt–Cu alloy system (*47*). The decreased integrated intensities and peak heights of bands due to CO adsorption on Pt as a function of increasing amounts of Au, seen in our study, might be due to the smaller number of Pt surface sites as more Au was added. This interpretation would agree with our chemisorption results. It is also important to determine whether there is any change in the apparent average molar extinction coefficient of the CO adsorption band with addition of Au, because this could influence the characteristics of adsorption. We will define the apparent average molar extinction coefficient using the notation of Ponec *et al.* (*13, 46*) as the ratio of the total integrated intensity of the CO adsorption band to the moles of adsorbed CO molecules as determined by chemisorption experiments. This value in units of 10^{-6} cm^{-1} mol^{-1} was 5.71, 6.19, and 6.72 for the 1.0 Pt/SiO_2, 1.0 Pt–0.3 Au/SiO_2, and 1.0 Pt–0.7 Au/SiO_2 catalysts, respectively. Clearly, the molar extinction coefficient as defined above did not change in a significant manner with the addition of Au.

Finally, one must consider the effect of electronic interaction between Pt and Au. To justify a shift to lower frequencies by electronic arguments, one would have to assume that the second metal component acts as an electron donor, thereby increasing the electron density of Pt sites in close proximity to the donor atoms. Shifting of the CO peak to lower frequencies could be caused by increased back-donation of electrons from *d*-orbitals of Pt to the antibonding $2\pi^*$ orbital of CO. However, such an electron donation from Au to Pt is not very likely due to the higher electronegativity of Au compared to Pt. Yet, we find that the peak corresponding to the total CO adsorption on Pt at room temperature is shifted from 2077 cm^{-1} for the monometallic Pt/SiO_2 catalyst to 2072 cm^{-1} for the bimetallic catalyst having 17 at.% Au and to 2060 cm^{-1} for the catalyst containing 30 at.% Au. These shifts are small enough to rationalize them in terms of geometric effects, where Au disrupts Pt ensembles causing a decrease in the dipole–dipole coupling of adsorbed CO molecules. This argument is similar to the ensemble effect postulated by Toolenaar *et al.* (*47*) for the supported Pt–Cu system and is consistent with the infrared results on other bimetallic systems (*13*). Previous TPD studies (*16, 48*) also did not indicate any noticeable electronic effect in the Pt–Au system.

Experimental evidence for a red shift induced by decreased dipole–dipole coupling comes from thermal desorption of CO from the 1.0 Pt/SiO_2 catalyst which had been saturated with CO at room temperature. We found that the peak resulting from linearly adsorbed CO on the reduced Pt surface shifted from 2077 cm^{-1} at room temperature to around 2052 cm^{-1} at 573 K. Increasing the temperature leads to smaller CO sur-

face coverage, and hence, to a decrease in the extent of dipole–dipole coupling of adsorbed CO.

Another interesting result is that the percentage of weakly held CO as determined from chemisorption (amount desorbed by 30 min of evacuation after saturation) does not change in a significant manner for the two bimetallic catalysts compared to the monometallic 1.0 Pt/SiO_2 catalyst, suggesting that the metal–CO bond strength does not change much with addition of Au. This result is in contrast to that reported for the $Pt–Sn/Al_2O_3$ and $Pt–Pb/Al_2O_3$ bimetallic systems (*49*). In those systems, an increase in reversibly held CO was found with increasing second metal content, and this was attributed to the weakening of the σ metal–CO bond. Such a change in σ bond strength could be due to effects other than geometric.

CONCLUSIONS

Adding Au to Pt/SiO_2 resulted in a decrease in Pt surface sites but did not significantly change the relative amounts of weakly held adsorbates (amount desorbed by 30 min evacuation at room temperature after initial chemisorption). Total uptake of hydrogen at room temperature was always somewhat higher than that of oxygen.

From the IR results in the $Pt–Au/SiO_2$ system, one can infer that the effects of Au are mainly geometric in nature. CO adsorbed on monometallic Pt/SiO_2 predominantly in a linear mode. Increasing the Au content caused a progressive shift of the linear CO band to lower frequencies. This shift can be rationalized in terms of decreased dipole–dipole coupling of adsorbed CO species. The total integrated intensity of the CO band decreased with increasing Au content, indicating fewer Pt sites exposed to the gaseous environment compared to the monometallic Pt/SiO_2 catalyst.

Subjecting the bimetallic samples to high-temperature oxidation/reduction cycles redispersed the Pt in the bimetallic catalyst with 17 at.% Au to a larger extent compared to that in the bimetallic catalyst containing 30 at.% Au. Previous electron microscopy characterization of the catalyst with 17 at.% Au revealed that most particles smaller than 20 nm were mainly elemental platinum, and larger particles were gold. In contrast, the catalyst with 30 at.% Au had smaller particles (<10 nm) which could be identified as Au_3Pt. In light of this, it is reasonable to expect that the catalyst having larger monometallic Pt particles (i.e., catalyst 1.0 Pt–0.3 Au having 17 at.% Au) would be more susceptible to redispersion than the other catalyst which contained smaller bimetallic particles.

ACKNOWLEDGMENT

Support for this work was provided by Grant CBT-8608106 from the National Science Foundation and is gratefully acknowledged.

REFERENCES

1. Pearson, W. B., "Handbook of Lattice Spacings and Structures of Metals and Alloys," p. 440, Pergamon Press, London, 1958.
2. Galvagno, S., and Parravano, G., *J. Catal.* **57,** 272 (1979).
3. Sachdev, A., and Schwank, J., *J. Catal.*, in press.
4. Bouwman, R., and Sachtler, W. M. H., *J. Catal.* **19,** 127 (1970).
5. Kuijers, F. J., Dessing, R. P., and Sachtler, W. M. H., *J. Catal.* **33,** 316 (1974).
6. Bouwman, R., *Gold Bull.* **11,** 3 (1978).
7. Hörnström, S. E., Johansson, L. I., and Flodström, A., *Appl. Surf. Sci.* **26,** 27 (1986).
8. Fukushima, T., Galvagno, S., and Parravano, G., *J. Catal.* **57,** 177 (1979).
9. Kugler, E. L., and Boudart, M., *J. Catal.* **59,** 201 (1979).
10. Soma-Noto, Y., and Sachtler, W. M. H., *J. Catal.* **32,** 316 (1974).
11. Hendrickx, H. A. C. M., and Ponec, V., *Surf. Sci.* **192,** 234 (1987).
12. Toolenaar, F. J. C. M., Reinalda, D., and Ponec, V., *J. Catal.* **64,** 110 (1980).
13. Bastein, A. G. T. M., Toolenaar, F. J. C. M., and Ponec, V., *J. Catal.* **90,** 88 (1984).
14. Palazov, A., Bonev, Ch., Kadinov, G., Shopov, D., Leitz, G., and Völter, J., *J. Catal.* **71,** 1 (1981).
15. De Jong, K. P., Bongenaar-Schlenter, B. E., Meima, G. R., Verkerk, R. C., Lammers, M. J. J., and Geus, J. W., *J. Catal.* **81,** 67 (1983).
16. Anderson, J. R., Foger, K., and Breakspere, R. J., *J. Catal.* **57,** 458 (1979).

17. Robbins, J. L., *J. Catal.* **115,** 120 (1989).
18. Haaland, D. M., *Surf. Sci.* **185,** 1 (1987).
19. Schwank, J., Parravano, G., and Gruber, H. L., *J. Catal.* **61,** 19 (1980).
20. Trapnell, B. M. W., *Proc. R. Soc. (London) A* **218,** 566 (1953).
21. Mikowski, R. J., Boudart, M., and Taylor, H. S., *J. Amer. Chem. Soc.* **76,** 3814 (1954).
22. Culver, R., Pritchard, J., and Tompkins, F. C., *in* "Proceedings, 2nd Int. Congr. Surf. Act.," Vol. 2, p. 243, 1957.
23. Pritchard, J., and Tompkins, F. C., *Trans. Faraday Soc.* **56,** 540 (1960).
24. Galvagno, S., Schwank, J., and Parravano, *J. Catal.* **69,** 283 (1981).
25. Palmer, Jr., M. B., and Vannice, M. A., *J. Chem. Technol. Biotechnol.* **30,** 205 (1980).
26. Tsuchiya, S., Amenomiya, Y., and Cvetanovic, R. J., *J. Catal.* **19,** 245 (1970).
27. Frennet, A., and Wells, P. B., *Appl. Catal.* **18,** 243 (1985).
28. Primet, M., Basset, J. M., Mathieu, M. V., and Prettre, M., *J. Catal.* **28,** 368 (1973).
29. Dixon, L. T., Barth, R., Gryder, J. W., *J. Catal.* **37,** 368 (1975).
30. O'Cinneide, A., and Gault, F. G., *J. Catal.* **37,** 311 (1975).
31. De Jongste, H. C., and Ponec, V., *J. Catal.* **64,** 228 (1980).
32. Gruber, H. L., *J. Phys. Chem.* **66,** 48 (1962).
33. Eischens, R. P., and Pliskin, W. A., *in* "Advances in Catalysis" (D. D. Eley, Herman Pines, and Paul B. Weisz, Eds.), Vol. 10, p. 1. Academic Press, New York, 1958.
34. Sinfelt, J. H., *J. Catal.* **28,** 308 (1973).
35. Wilson, G. R., and Hall, W. K., *J. Catal.* **17,** 190 (1970).
36. Bassi, I. W., Garbassi, F., Vlaic, G., Marzi, A., Tauszik, G. R., Cocco, G., Galvagno, S., and Parravano, G., *J. Catal.* **64,** 405 (1980).
37. Bartók, M., Sárkány, J., and Sitkei, A., *J. Catal.* **72,** 236 (1981).
38. Barth, R., Pitchai, R., Anderson, R. L., and Verykios, X. E., *J. Catal.* **116,** 61 (1989).
39. Primet, M., Basset, J. M., Mathieu, M. V., and Prettre, M., *J. Catal.* **29,** 213 (1973).
40. Sárkány, J., Bartók, M., and Gonzalez, R. D., *J. Catal.* **81,** 347 (1983).
41. Stoop, F., Toolenaar, F. J. C. M., and Ponec, V., *J. Catal.* **73,** 50 (1982).
42. Kottke, M. L., Greenler, R. G., and Tomkins, H. G., *Surf. Sci.* **32,** 231 (1972).
43. Yates, D. J. C., *J. Colloid Interface Sci.* **29,** 194 (1969).
44. Solomennikov, A. A., Lokhov, Y. A., Davydov, A. A., and Ryndin, Y. A., *Kinet. Katal.* **20,** 714 (1979).
45. Blyholder, G., *J. Phys. Chem.* **68,** 2772 (1964).
46. Toolenaar, F. J. C. M., Bastein, A. G. T. M., and Ponec, V., *J. Catal.* **82,** 35 (1983).
47. Toolenaar, F. J. C. M., Stoop, F., and Ponec, V., *J. Catal.* **82,** 1 (1983).
48. Sachtler, J. W. A., Somorjai, G. A., *J. Catal.* **81,** 77 (1983).
49. Palazov, A., Bonev, Ch., Shopov, D., Lietz, G., Sárkány, A., and Völter, J., *J. Catal.* **103,** 249 (1987).